

Research Paper

Competitive Performance of Carbon “Quantum” Dots in Optical Bioimaging

Li Cao, Sheng-Tao Yang, Xin Wang, Pengju G. Luo, Jia-Hui Liu, Sushant Sahu, Yamin Liu, Ya-Ping Sun 

Department of Chemistry and Laboratory for Emerging Materials and Technology, Clemson University, Clemson, South Carolina 29634-0973, USA.

 Corresponding author: Tel: 864-656-5026, Fax: 864-656-6613, E-mail: syaping@clemson.edu

© Ivyspring International Publisher. This is an open-access article distributed under the terms of the Creative Commons License (<http://creativecommons.org/licenses/by-nc-nd/3.0/>). Reproduction is permitted for personal, noncommercial use, provided that the article is in whole, unmodified, and properly cited.

Received: 2011.12.04; Accepted: 2012.01.01; Published: 2012.03.07

Abstract

Carbon-based “quantum” dots or carbon dots are surface-functionalized small carbon nanoparticles. For bright fluorescence emissions, the carbon nanoparticles may be surface-doped with an inorganic salt and then the same organic functionalization. In this study, carbon dots without and with the ZnS doping were prepared, followed by gel-column fractionation to harvest dots of 40% and 60% in fluorescence quantum yields, respectively. These highly fluorescent carbon dots were evaluated for optical imaging in mice, from which bright fluorescence images were obtained. Of particular interest was the observed competitive performance of the carbon dots *in vivo* to that of the well-established CdSe/ZnS QDs. The results suggest that carbon dots may be further developed into a new class of high-performance yet nontoxic contrast agents for optical bioimaging.

Key words: Carbon dots, fluorescence, optical bioimaging, quantum dots.

1. Introduction

Small carbon nanoparticles have been shown as versatile precursors for brightly fluorescent nano-dots [1-15], with the observed optical properties in solution phenomenologically similar to and performance-wise comparable with those of the well-established semiconductor quantum dots (QDs) [9, 16-19]. Structurally, the fluorescent carbon-based “quantum” dots (or often referred to as carbon dots) are small carbon nanoparticles with relatively simple particle surface functionalization [1,2,7,10,11]. Carbon dots with oligomeric polyethylene glycol diamine (PEG_{1500N}, Scheme 1/Figure S1) [20] as the surface functionalization agent were shown to be nontoxic [21], amenable to fluorescence bioimaging applications *in vitro* and *in vivo* [10,11,22,23]. More recently, highly fluorescent carbon dots with emission quantum yields more than 50% were obtained by surface-doping the core carbon nanoparticles with an inorganic salt such as ZnS (Scheme 1/Figure S1) or TiO₂ [20,24], and/or by ap-

plying a gel-column fractionation scheme to the as-synthesized carbon dots samples [9,20]. The brighter dots thus harvested promise more and better opportunities for fluorescence bioimaging, especially for uses *in vivo* to improve the contrast against tissue background. Here we report an experimental validation on the use of these highly fluorescent carbon dots for imaging in mice, with especially a demonstration on the competitive performance of these dots to that of the well-established semiconductor QDs under purposely matching experimental conditions.

2. Experimental Section

2.1. Materials

Carbon nano-powders, *O,O'*-bis(3-aminopropyl) polyethylene glycol ($M_w \sim 1,500$, PEG_{1500N}) and thionyl chloride (>99%) were purchased from Aldrich, zinc acetate dihydrate (Zn(OOCC₂H₅)₂•2H₂O, >98%) and sodium sulfide (Na₂S•9H₂O, >98%) from Alfa,

and nitric acid, *N,N*-dimethylformamide (DMF, 99%), and sodium dodecyl sulfate (SDS, 99%) from VWR. The aqueous CdSe/ZnS quantum dots solution (Qdot® 525 ITK™ amino (PEG) QDs) was acquired from Invitrogen. Millipore Durapore membrane filters (pore size 0.22 μm) and dialysis membrane tubing were supplied by Spectrum Laboratories. Water was deionized and purified by being passed through a Labconco WaterPros water purification system.

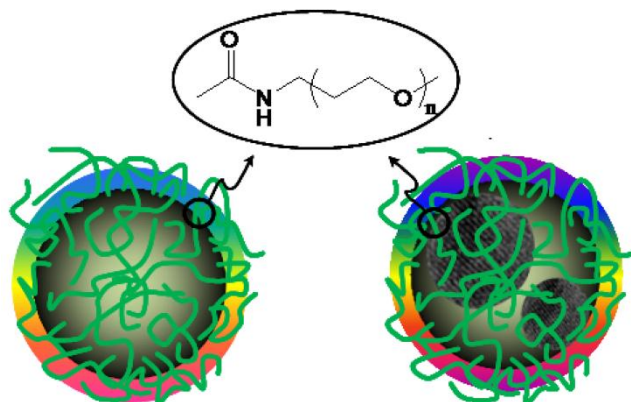


Figure S1. (Scheme 1) Cartoon illustrations of non-doped (left) and doped (right) carbon dots [20].

2.2. Measurement

Baxter Megafuge (model 2630) and Beckman-Coulter ultracentrifuge (Optima L90K with a type 90 Ti fixed-angle rotor) were used. UV/vis absorption spectra were recorded on a Shimadzu UV2101-PC spectrophotometer. Fluorescence spectra were measured on a Jobin-Yvon emission spectrometer equipped with a 450 W xenon source, Gemini-180 excitation and Tirax-550 emission monochromators, and a photon counting detector (Hamamatsu R928P PMT at 950 V). Quinine sulfate and 9,10-bis(phenylethynyl)-anthracene were used as standards in the determination of fluorescence quantum yields by the relative method (matching the absorbance at the excitation wavelength between the sample and standard solutions and comparing their corresponding integrated total fluorescence intensities). Atomic force microscopy (AFM) images were acquired in the acoustic AC mode on a Molecular Imaging PicoPlus AFM system equipped with a multipurpose scanner and a NanoWorld point probe NCH sensor. Transmission electron microscopy (TEM) characterization was carried out on Hitachi 9500 TEM and Hitachi HD-2000 S-TEM systems. Confocal fluorescence images were obtained on a Leica laser scanning confocal fluorescence microscope

(DM IRE2, with Leica TCS SP2 SE scanning system) equipped with an argon ion laser (JDS Uniphase). The fluorescence imaging in mice was performed on a MAG Biosystems Lumazone FA in vivo Imaging System equipped with an Asahi Max-301 xenon arc source for excitation through a liquid light guide and a Princeton Instruments PIXIS:1024B digital CCD camera system as detector. Band-pass and cut-off filters were used for the selection of excitation and emission wavelengths.

2.3. Carbon Dots

A carbon nano-powder sample (2 g) was refluxed in an aqueous nitric acid solution (2.6 M, 200 mL) for 12 h. The mixture back at room temperature was dialyzed against fresh water, followed by centrifuging at 1,000g to retain the supernatant. The surface-oxidized small carbon nanoparticles recovered from the supernatant (100 mg) were refluxed in neat thionyl chloride for 6 h. Upon the removal of excess thionyl chloride on a rotary evaporator with a vacuum pump, the sample was mixed well with PEG_{1500N} (1 g) in a flask. The mixture was heated to 110 °C, and vigorously stirred at that temperature under nitrogen protection for 3 days. The sample back at room temperature was dispersed in water, followed by centrifuging at 25,000g to retain the supernatant as an aqueous solution of the as-prepared carbon dots. The sample solution was concentrated and then loaded onto a Sephadex G-100™ gel-column packed in house for fractionation [9]. Fluorescence quantum yields of the fractions were determined, and those more fluorescent were combined into a single aqueous solution of carbon dots (40% in fluorescence quantum yield) for further characterization and bioimaging.

For the surface-doping with ZnS, the surface-oxidized carbon nanoparticles (600 mg) were dispersed in DMF (200 mL) *via* sonication for 30 min, and to the suspension was first added Zn(OOCCH₃)₂•2H₂O (680 mg, 3.1 mmol) under vigorous stirring and then slow dropwise addition of an aqueous Na₂S solution (0.62 M, 5 mL) at room temperature. The mixture was centrifuged at 3,000g, and the precipitate was retained and repeatedly washed with distilled water to obtain the ZnS-doped carbon nanoparticles (881 mg).

The ZnS-doped carbon nanoparticles (200 mg) were dispersed in an aqueous SDS solution (1 wt%, 120 mL) *via* sonication for 30 min. Upon filtration, the filter cake was washed repeatedly with water and then dried. The solid sample was mixed thoroughly with PEG_{1500N} (1.9 g), and the mixture was heated to 110 °C and stirred at that temperature for 72 h under nitrogen protection. The reaction mixture back at

room temperature was dispersed in water, followed by centrifuging at 25,000g to retain the supernatant as an aqueous solution of as-prepared C_{ZnS} -Dots. The sample solution was similarly concentrated and then fractionated on the same Sephadex G-100TM gel-column [20]. Fluorescence quantum yields of the fractions were determined, and those more fluorescent were combined into a single aqueous solution of C_{ZnS} -Dots (60% in fluorescence quantum yield) for further characterization and bioimaging.

2.4. Imaging in Mice

All of the animal experiments were performed at Clemson University by strictly following the IACUC (Institutional Animal Care and Use Committee) approved protocols. Female DBA/1 mice (~25 g, acquired from Harlan) were housed in plastic cages (three mice/cage) at the Godley-Snell Research Center at Clemson University and kept on a 12 h light/dark cycle, with food and water provided *ad libitum*. Following the acclimation of one week, the mice were randomly divided into groups of 3 mice per group for imaging evaluations. Throughout the imaging experiments the mice were kept under anaesthesia (3% isoflurane flow). Two injection modes (subcutaneous and front extremity) were used for the *in vivo* imaging. Before subcutaneous injection, the back area surrounding the injection point on the mouse was shaved to minimize autofluorescence. The control group in both injection modes was injected with equivalent volume of phosphate buffered saline (PBS). For the front extremity injection, the mice 24 h post-injection were sacrificed by CO₂ treatment under anaesthesia. The axillary lymph nodes were dissected for fluorescence imaging. All images were processed and analyzed by using the NIH-commissioned and supplied ImageJ software (<http://rsbweb.nih.gov/ij/>).

3. Results and Discussion

Small carbon nanoparticles (mostly less than 10 nm in diameter) were harvested from the commercially supplied carbon nano-powders (Aldrich) by first the aqueous nitric acid treatment and then a combination of dialysis to remove impurities and vigorous centrifuging to retain the supernatant. These nanoparticles were functionalized with PEG_{1500N} in classical amidation reaction to yield PEGylated carbon dots (Scheme 1/Figure S1). The as-prepared sample was fractionated on a gel-column (SephadexTM G-100) to harvest the more fluorescent portion of the sample [9], with the corresponding fluorescence quantum yield in the green of 40% (440 nm excitation, figure 1).

The sample solution was diluted for the preparation of specimens for characterization by microscopy techniques. Both AFM and TEM results showed dot-like images (figure 2), agreeing well with those for carbon dots reported previously [9].

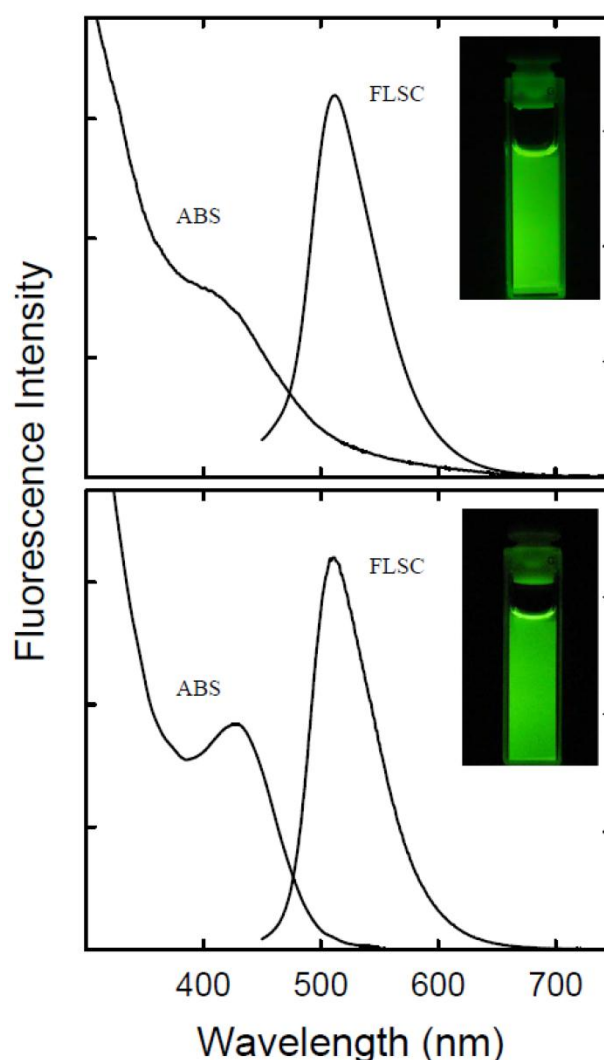


Figure 1. Absorption (ABS) and fluorescence (FLSC, 440 nm excitation) spectra of the carbon dots without (upper) and with the ZnS doping (lower) in aqueous solutions, with fluorescence quantum yields of 40% and 60%, respectively. In the insets are photos of the corresponding solutions (excitation at 440 nm and emissions monitored through a 530 nm cut-off filter).

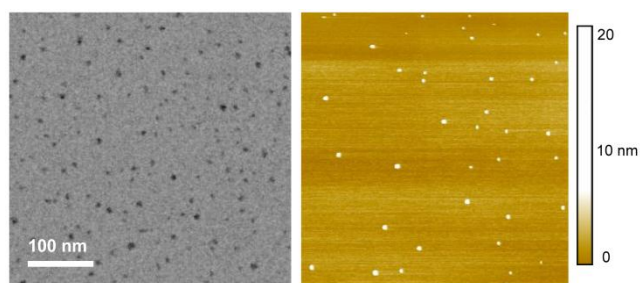


Figure 2. TEM (left) and AFM (right) images of the carbon dots (without ZnS doping) used in the optical imaging experiments.

The carbon nanoparticles could be suspended in aqueous solution in a relatively stable fashion, thus serving as nucleation centers in the titration of zinc acetate with sodium sulfide for the formation of ZnS to yield ZnS-doped carbon nanoparticles [24]. The surface-doping level likely varied from particle to particle, so that a surfactant (sodium dodecyl sulfate or SDS)-assisted dispersion procedure in favor of the carbon nanoparticles with more ZnS doping was used to exclude those with no or a negligible level of doping. Subsequently, those nanoparticles with the surface completely covered by ZnS (thus no accessible carboxylic acid moieties on the particle surface for reactions with amino molecules) were discriminated in the functionalization chemistry with PEG_{1500N} [20]. The functionalization reaction conditions were similar to those used for carbon dots without the surface doping, resulting in ZnS-doped carbon dots (denoted

as C_{ZnS}-Dots). According to thermogravimetric analysis (TGA), the estimated core composition in terms of C:ZnS molar ratio in the C_{ZnS}-Dots was about 20:1. The as-prepared sample was similarly fractionated on the gel-column to harvest more fluorescent C_{ZnS}-Dots [20], with the observed fluorescence quantum yield in the green of 60% (440 nm excitation, figure 1). These dots were diluted for the preparation of specimens for characterization by AFM and TEM, and the representative results are shown in figure 3. The vigorously diluted solution was also used to disperse the dots on cover-glass surface for confocal fluorescence imaging under the same specimen and measurement conditions as those for commercially supplied CdSe/ZnS QDs (Invitrogen Qdot® 525 ITK™ amino (PEG) QDs, fluorescence quantum yield ~60% verified). As shown in figure 4, the well-dispersed C_{ZnS}-Dots and the CdSe/ZnS QDs are quite similar in fluorescence brightness at essentially the individual dot level.

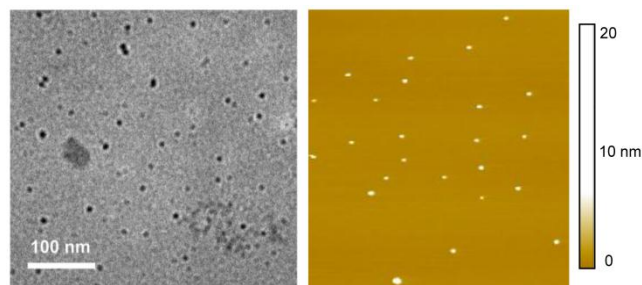


Figure 3. Representative TEM (left) and AFM (right) images of the ZnS-doped carbon dots (C_{ZnS}-Dots) used in the optical imaging experiments.

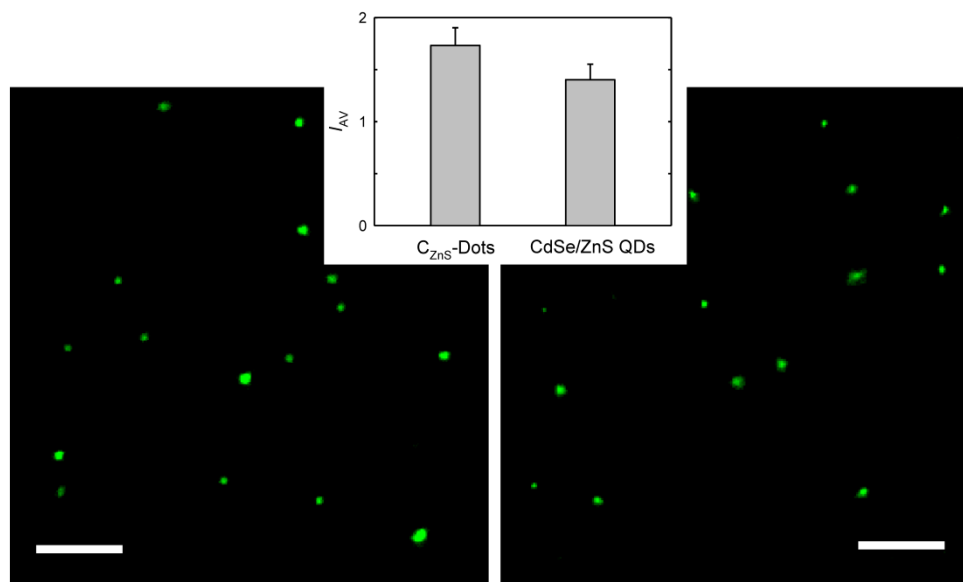


Figure 4. Confocal fluorescence images (458 nm excitation, 10 μ m for the scale bars) of the C_{ZnS}-Dots (left) and the commercially supplied CdSe/ZnS QDs (right). In the inset is a comparison on the average image intensity (I_{AV}) for 60 dots between the two specimens.

The highly fluorescent carbon dots without and with the ZnS doping (quantum yields 40% and 60%, respectively) were evaluated in terms of fluorescence imaging in mice [23]. The animal experiments were performed by strictly following the IACUC (Institutional Animal Care and Use Committee) approved protocols. Female DBA/1 mice (~25 g) were housed in plastic cages (three mice/cage) at the Godley-Snell Research Center for animal research at Clemson University on a 12 h light/dark cycle and provided with food and water *ad libitum*. Following the acclimation of one week, the mice were randomly divided into groups of three mice per group. For the injection and subsequent imaging, the mice were kept under anesthesia with 3% isoflurane flow.

Before the subcutaneous injection, the back area surrounding the injection point on the mouse was

shaved to avoid autofluorescence. The injection volume was kept at 20 μ L, with the solution concentration adjusted to match the targeted optical density at the excitation wavelength. As shown in figure 5, fluorescence emissions from the subcutaneously injected dots could readily be detected in a Lumazone FA *in vivo* imaging system (MAG Biosystems), with a relatively shorter fluorescence collection time and improved imaging contrast in comparison with those in the use of as-prepared less fluorescent carbon dots [23]. The image brightness was obviously higher for the C_{ZnS}-Dots sample, consistent with the corresponding higher fluorescence quantum yield in solution. In mice the subcutaneously injected carbon dots diffused relatively slowly, with the gradual fading of fluorescence signals in about 24 h post-injection.

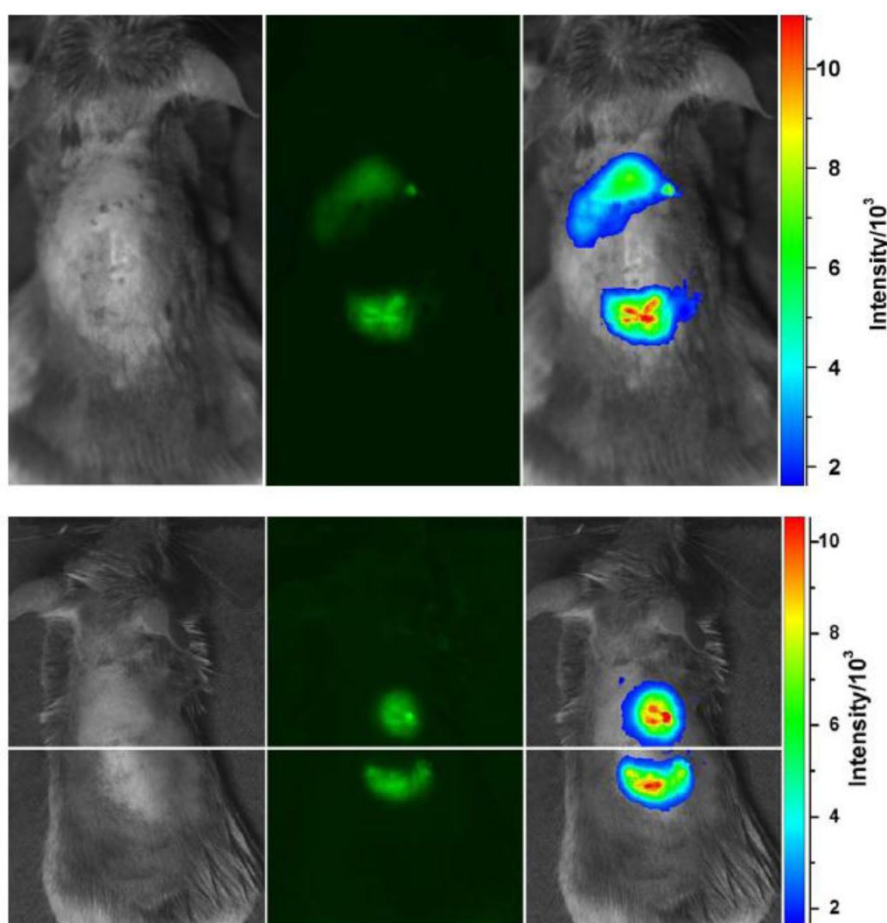


Figure 5. Top: Subcutaneously injected carbon dots (upper spot) and C_{ZnS}-Dots (lower spot) of similar optical densities in mice (470 nm and 525 nm band-pass filters for excitation and emission, respectively). Bottom: Subcutaneously injected C_{ZnS}-Dots (upper spot) and Invitrogen Qdot® 525 ITK™ amino (PEG) QDs (lower spot) of similar optical densities in mice (434 nm band-pass filter for excitation and 474 nm cut-off filter for emission collection). The color-coded images (right) were processed with ImageJ from NIH.

In a comparison of fluorescence imaging performance with commercially supplied CdSe/ZnS QDs (Invitrogen Qdot® 525 ITK™ amino (PEG) QDs), the concentration of the subcutaneously injected QDs was adjusted such that the optical density was approximately the same as that of the carbon dots *in vivo*. The resulting fluorescence images for C_{ZnS}-Dots and the CdSe/ZnS QDs in mice were of similar brightness (figure 5), consistent with their similar fluorescence quantum yields in solution and comparable fluorescence imaging results at the individual dot level (figure 4).

For potential uses of carbon dots for fluorescence imaging *in vivo*, a relatively straightforward demonstration is on tracking the migration of the dots through lymph vessels in mice following the paw injection [23,25,26]. For the highly fluorescent carbon dots without and with ZnS doping (quantum yields 40% and 60%, respectively), they could both migrate along the arm upon their intradermal injection into the front extremity (figure 6). However, the migration of the C_{ZnS}-Dots was apparently less pronounced, with the relative brightness in the fluorescence images

(figure 6) of the migrated dots suggesting less C_{ZnS}-Dots (more fluorescent) migrated. The axillary lymph nodes were harvested and dissected at 24 h post-injection, where strong fluorescence emissions from the carbon dots were observed (figure 6), further confirming the migration of the dots and the preservation of their fluorescence properties *in vivo*.

The improved optical imaging performance of these more fluorescent carbon dots in mice further confirms that the excellent fluorescence properties of carbon dots observed in solutions and on surface at the individual dot level are preserved *in vivo*, suggesting significant application potentials of carbon dots. Particularly encouraging is the fact that the *in vivo* performance of the carbon dots is competitive to that of the well-established CdSe/ZnS QDs, beyond the obvious advantage of carbon dots being nontoxic according to available experimental evaluations [10,11,21,27-29]. The results from this study justify the further development of carbon dots into a new class of high-performance yet benign contrast agents for optical bioimaging.

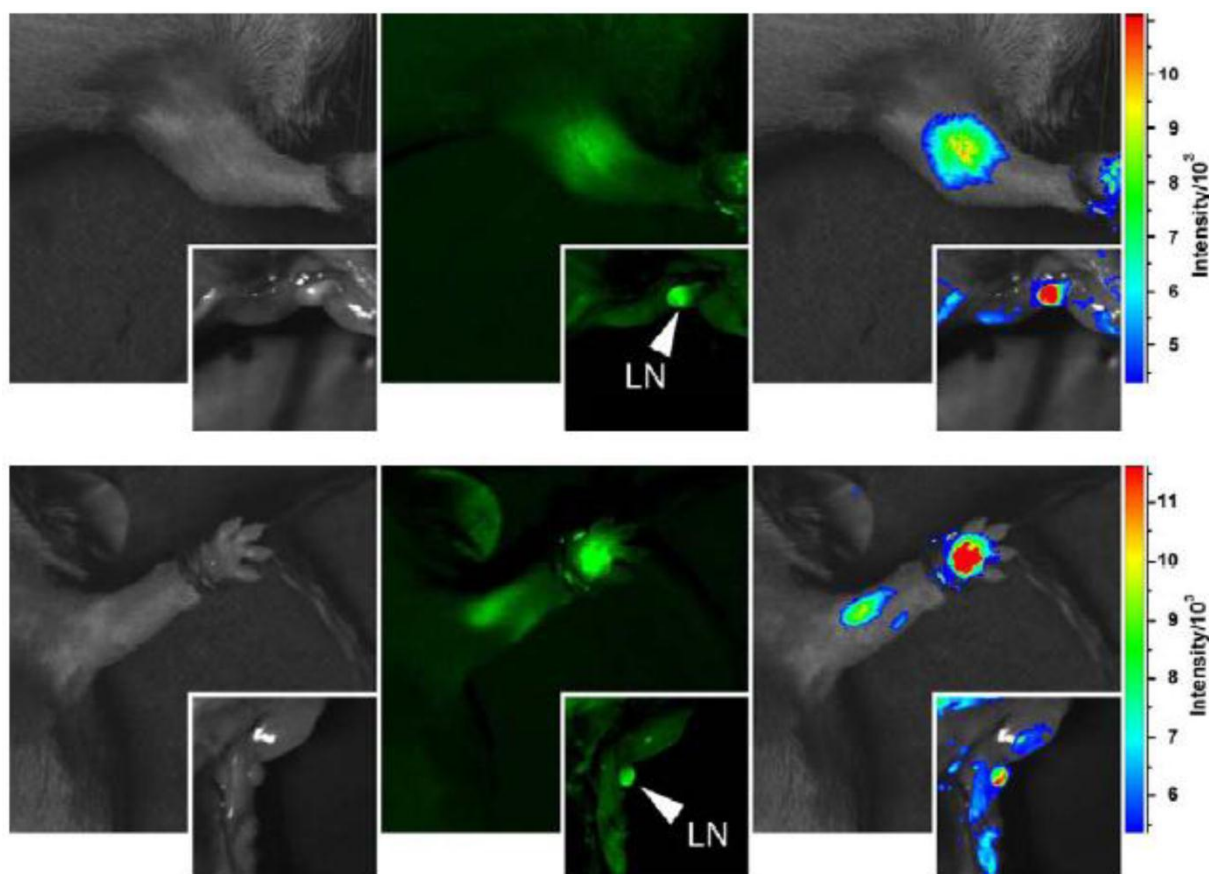


Figure 6. Intradermally injected carbon dots (upper) and C_{ZnS}-Dots (lower) of similar optical densities in mice, with images of dissected lymph nodes in the insets (470 nm and 525 nm band-pass filters for excitation and emission, respectively). The color-coded images (right) were processed with ImageJ from NIH.

Acknowledgment

This work was initiated and supported by funding from NIH and then from NSF. L.C. was supported by a *Susan G. Komen for the Cure* Postdoctoral Fellowship. S.S. was a participant supported by Palmetto Academy, an education-training program managed by South Carolina Space Grant Consortium.

Conflict of Interest

The authors have declared that no conflict of interest exists.

References

1. Sun Y-P, Zhou B, Lin Y, et al. Quantum-sized carbon dots for bright and colorful photoluminescence. *J. Am. Chem. Soc* 2006; 128: 77561. -7757.
2. Cao L, Wang X, Mezziani MJ, et al. Carbon dots for multiphoton bioimaging. *J. Am. Chem. Soc* 2007; 129: 11318-11319.
3. Bourlino AB, Stassinopoulos A, Anglos D, et al. Surface functionalized carbogenic quantum dots. *Small* 2008; 4: 455-458.
4. Bourlino AB, Stassinopoulos A, Anglos D, et al. Photoluminescent carbogenic dots. *Chem. Mater* 2008; 20: 4539-4541.
5. Tian L, Ghosh D, Chen W, et al. Nanosized carbon particles from natural gas soot. *Chem. Mater* 2009; 21: 2803-2809.
6. Hu S-L, Niu K-Y, Sun J, et al. One-step synthesis of fluorescent carbon nanoparticles by laser irradiation. *J. Mater. Chem* 2009; 19: 484-488.
7. Peng H, Trivas-Sejdic J. Simple aqueous solution route to luminescent carbogenic dots from carbohydrates. *Chem. Mater* 2009; 21: 5563-5565.
8. Jiang HQ, Chen F, Kagally MG, Denes FS. New strategy for synthesis and functionalization of carbon nanoparticles. *Langmuir* 2010; 26: 1991-1995.
9. Wang X, Cao L, Yang S-T, et al. Bandgap-like strong fluorescence in functionalized carbon nanoparticles. *Angew. Chem. Int. Ed* 2010; 49: 5310-5314.
10. Li Q, Ohulchanskyy TY, Liu RL, et al. Photoluminescent carbon dots as biocompatible nanoprobe for targeting cancer cells in vitro. *J. Phys. Chem. C* 2010; 114: 12062-12068.
11. Qiao Z-A, Wang Y, Gao Y, et al. Commercially activated carbon as the source for producing multicolor photoluminescent carbon dots by chemical oxidation. *Chem. Commun* 2010; 46: 8812-8814.
12. Li H, He X, Liu Y, et al. One-step ultrasonic synthesis of water-soluble carbon nanoparticles with excellent photoluminescent properties. *Carbon* 2011; 49: 605-609.
13. Li H, He X, Liu Y, et al. Synthesis of fluorescent carbon nanoparticles directly from active carbon via a one-step ultrasonic treatment. *Mater. Res. Bull* 2011; 46: 147-151.
14. Li X, Wang H, Shimizu Y, et al. Preparation of carbon quantum dots with tunable photoluminescence by rapid laser passivation in ordinary organic solvents. *Chem. Commun* 2011; 47: 932-934.
15. Wang F, Pang S, Wang L, et al. One-step synthesis of highly luminescent carbon dots in noncoordinating solvents. *Chem. Mater* 2010; 22: 4528-4530.
16. Alivisatos AP. Semiconductor clusters, nanocrystals, and quantum dots. *Science* 1996; 271: 933-937.
17. Bruchez M, Moronne M, Gin P, et al. Semiconductor nanocrystals as fluorescent biological labels. *Science* 1998; 281: 2013-2016.
18. Wu X, Liu H, Liu J, et al. Immunofluorescent labeling of cancer marker Her2 and other cellular targets with semiconductor quantum dots. *Nat. Biotechnol* 2003; 21: 41-46.
19. Resch-Genger U, Grabolle M, Cavaliere-Jaricot S, et al. Quantum dots versus organic dyes as fluorescent labels. *Nat. Methods* 2008; 5: 763-775.
20. Anilkumar P, Wang X, Cao L, et al. Toward quantitatively fluorescent carbon-based "quantum" dots. *Nanoscale* 2011; 3: 2023-2027.
21. Yang S-T, Wang X, Wang H, et al. Carbon dots as nontoxic and high-performance fluorescence imaging agents. *J. Phys. Chem. C* 2009; 113: 18110-18114.
22. Liu R, Wu D, Liu S, et al. An aqueous route to multicolor photoluminescent carbon dots using silica spheres as carriers. *Angew. Chem. Int. Ed* 2009; 48: 4598-4601.
23. Yang S-T, Cao L, Luo P, et al. Carbon dots for optical imaging in vivo. *J. Am. Chem. Soc* 2009; 131: 11308-11309.
24. Sun Y-P, Wang X, Lu F, et al. Doped carbon nanoparticles as a new platform for highly photoluminescent dots. *J. Phys. Chem. C* 2008; 112: 18295-18298.
25. Kim S, Lim YT, Soltesz EG, et al. Near-infrared fluorescent type II quantum dots for sentinel lymph node mapping. *Nat. Biotechnol* 2004; 22: 93-97.
26. Ballou B, Ernst LA, Andreko S, et al. Sentinel lymph node imaging using quantum dots in mouse tumor models. *Bioconjug Chem* 2007; 18: 389-396.
27. Zhao Q-L, Zhang Z-L, Huang B-H, et al. Facile preparation of low cytotoxicity fluorescent carbon nanocrystals by electrooxidation of graphite. *Chem. Commun* 2008; 5116-5118.
28. Ray SC, Saha A, Jana NR, Sarkar R. Fluorescent carbon nanoparticles: Synthesis, characterization, and bioimaging application. *J. Phys. Chem. C* 2009; 113: 18546-18551.
29. Liu J-H, Anilkumar P, Cao L, et al. Cytotoxicity evaluations of fluorescent carbon nanoparticles. *Nano Life* 2010; 1: 153-161.